First-principles calculation of the electronic structure and EELS spectra at the graphene/Ni(111) interface

Giovanni Bertoni, Lionel Calmels, Anne Altibelli, and Virginie Serin
CEMES-CNRS, 29 Rue J. Marvig, BP 94347, 31055 Toulouse Cedex 4, France
(Received 14 September 2004; published 3 February 2005)

A spin-polarized first-principles calculation of the atomic and electronic structure of the graphene/Ni(111) interface is presented. Different structural models have been considered, which differ in the positions of the carbon atoms with respect to the nickel topmost layer. The most probable structure, which has the lowest energy, has been determined. The distance between the floating carbon layer and the nickel surface is found smaller than the distance between graphene sheets in bulk graphite, in accordance with experimental measurements. The electronic structure of the graphene layer is strongly modified by interaction with the substrate and the magnetic moment of the surface nickel atoms is lowered in the presence of the graphene layer. Several interface states have been identified in different parts of the interface two-dimensional Brillouin zone. Their influence on the electron energy loss spectra has been evaluated.

DOI: 10.1103/PhysRevB.71.075402 PACS number(s): 68.43.Fg, 73.20.At, 75.70.Ak, 79.20.Uv

I. INTRODUCTION

Graphene consists of a single graphite layer with strong covalent bonds between carbon atoms arranged in a honeycomb lattice. The nearest neighbor distance in the graphene layer (1.42 Å) is very close to the characteristic distance of the Ni(111) surface $a_{Ni}/\sqrt{6}=1.44$ Å, where $a_{Ni}=3.52$ Å is the measured lattice parameter for fcc nickel. The small difference between these two distances explains why a single sheet of graphene can be grown on the Ni(111) surface with perfect order at the interface. This two-dimensional system is interesting from a fundamental point of view because the electronic and magnetic structure of both nickel and graphene may change at the interface, but also because the graphene/Ni(111) interface can be considered as the simplest model system to explain the properties of more complex carbon/metal interfaces. Examples of these interfaces can be found in intercalated graphite,[1] incommensurate transition metal/graphene,[2] and carbide/graphene interfaces[3] or in filled fullerenes and nanotubes[4,5] for which curvature effects may be important and modify the interaction between the filling metal and the carbon graphitic coverage.

Epitaxial layers of graphene on Ni(111) have been obtained recently by decomposition of ethylene at temperatures higher than 900 K.[1,6,7] Electron diffraction studies have confirmed that the carbon overlayer is well ordered and possesses the 3*m* symmetry of the Ni(111) substrate.[1,6] Three different models, which preserve this 3*m* symmetry, can be considered for the adsorption sites of carbon atoms. Rosei *et al.*[8] have proposed a model where the carbon atoms occupy all the hollow sites of the nickel surface (the so-called hcp hollow sites just above the atoms of the second nickel layer and the fcc hollow sites above the atoms of the third nickel layer). In this model, shown as model A in Fig. 1, the carbon layer is floating at 2.80 Å over the topmost nickel layer and the distance between the nickel layers is the same as for the bulk metal, as deduced from surface sensitive Electron Energy Loss Spectroscopy (EELS) experiment.[8] The electronic structure for this model has first been calculated by Souzu and Tsukada.[9] Their calculation shows that the band structure for the nickel substrate is not modified in presence of the carbon overlayer while the graphene π-bands change significantly due to the overlapping of the graphene π-orbitals and substrate *d*-bands. This overlapping is responsible for a gap opening near the *K* point of the surface Brillouin zone and a mixing of the graphene π-orbitals with the nickel *d*-bands. Yamamoto *et al.* have studied a 22 atoms cluster ($C_6H_6Ni_{10}$) with the same interatomic distances as for model A. Their calculation concludes in a charge transfer from the metal to the graphene, due to occupied cluster hybridised orbitals which result from the overlapping of nickel and graphene orbitals of nearly the same energy.[10] These two theoretical

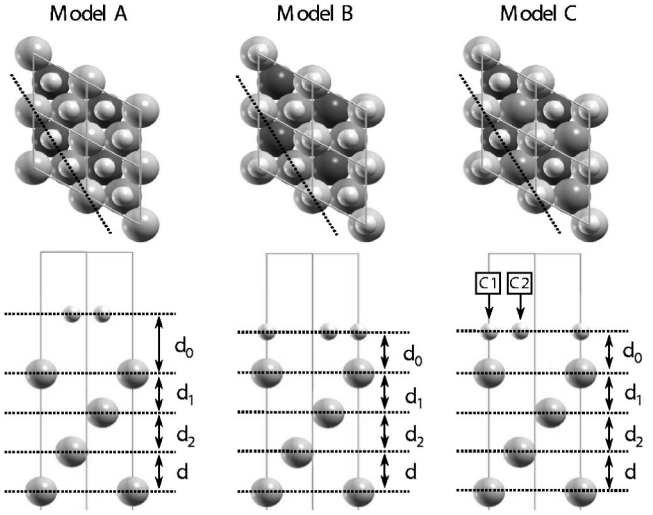

FIG. 1. The three possible models with 3*m* symmetry for the graphene/Ni(111) interface. Top: top view (the Ni atoms are represented by big spheres and are colored with darker grey as their distance from the interface increases, the carbon atoms are represented by small spheres). Bottom: side view in the plane indicated by a dotted line in the top views. For the values of the distances d_0, d_1, and d_2, see Table I. The two nonequivalent carbon atoms C_1 and C_2 are indicated for model C.

studies of model A neglect the magnetic polarization of the nickel substrate. Gamo *et al.* have proposed two alternative models for which half of the carbon atoms are located just above the interface nickel atoms, while the other carbon atoms are located either in the hcp hollow sites (model B of Fig. 1) or in the fcc hollow sites (model C of Fig. 1).[6] They concluded from Low Energy Electron Diffraction (LEED) measurements that model C is the most favorable with a distance of 2.11 Å and 2.16 Å between the nickel substrate and the two nonequivalent carbon atoms of the graphene overlayer. The buckling measured in this study (0.05 Å) is smaller than the estimated error (about 0.07 Å). This result has further been confirmed by an Impact Collision Ion Scattering Spectroscopy (ICISS) experiment[7] where a distance of 2.1 Å has been measured between the overlayer and the substrate. The electronic structure of the graphene/Ni(111) interface has never been studied in a first principles spin polarized calculation. Moreover, it would be interesting to compare the electronic structure of this interface with that of the *h*-BN/Ni(111) interface because graphite is a semimetal while *h*-BN is an insulator. Grad *et al.* have studied the *h*-BN/Ni(111) interface in a spin-polarized calculation. They found that the interface induces a reduction of the nickel magnetic moment and is responsible for a spin-dependant shift of the *h*-BN π-band.[11]

In the present paper, a spin-polarized calculation for the three models of the graphene/Ni(111) interface is presented. The results concern the structural relaxation, the magnetic moment of the Ni atoms and the electronic structure of the interface. Particular attention is given to the EELS study and we present results for the calculated carbon *K*-edge. Indeed, the continuous progresses of electron transmission techniques with an ultimate lateral resolution of a few angstroms allow the investigation of the electronic structure and its local modifications at an interface.[12–14] Our paper is organized as follows: in Sec. II we give a rapid description of the theoretical methods that have been used in our calculations. In Sec. III we describe the three different atomic structures that describe the interface. For each of these structures, we calculate the atomic positions and we show which structure has the lowest energy. Section IV gives result for the electronic and magnetic structure near the interface. In Sec. V we describe how the EELS carbon *K*-edge spectra are modified by interactions with the nickel substrate and finally we conclude in Sec. VI.

II. FIRST PRINCIPLES METHOD

We performed the self-consistent calculation of the total energy and charge, as well as the determination of the electronic and atomic structure, using a relativistic "full-potential" method based on "augmented-plane-waves +local orbitals" (APW+lo) as implemented in the WIEN2k code.[15] This code uses a basis of wave functions, which is very efficient for solving the Kohn-Scham equation in the density functional theory (DFT) framework. The exchange and correlation potential was treated in a generalized gradient approximation (GGA) in the parameterization of Perdew, Burke, and Ernzerhof.[16] We used atomic sphere radii of 2.2 a.u. for nickel atoms and 1.3 a.u. for carbon atoms. For the fundamental parameter $RK_{\max}$ (product of the smallest muffin-tin radius by the largest wave-vector used in the plane wave expansion) we used $RK_{\max}=8.5$ to calculate the electronic structure of the Ni(111) surface and $RK_{\max}=5.0$ to study the graphene/Ni(111) interface. These choices ensure an equal energy cut-off of about 15 Ry for all the systems. The basis of standard local orbitals which was used to describe the valence states was augmented with additional local orbitals for a better description of the semicore 3*p* states of nickel and the 2*s* states of carbon. The irreducible wedge of the two-dimensional Brillouin zone (2D-BZ) was sampled with a *k*-mesh of 102 points. This mesh is generated with a special grid used in the modified tetrahedron integration.[15] The surface and interfaces were modelled using symmetric slab cells periodically repeated in the whole space, with a vacuum separation of 22 a.u. for the clean surface, reduced to 15-16 a.u. after adding the graphene overlayer (we took the same cell size for all the systems). We used a slab of 13 layers of nickel, large enough for reducing interaction effects between the successive surfaces. Nicolay *et al.* have shown that such a large slab is necessary to avoid the effect of artificial splitting of the surface states.[17]

III. ATOMIC STRUCTURE OF THE GRAPHENE/Ni(111) INTERFACE

In order to find the most stable interface atomic structure, we have performed a self-consistent calculation for the three possible geometries (models A, B, and C) shown in Fig. 1. Structure relaxation was allowed in the [111] direction by minimizing the forces acting on the atoms of the graphene overlayer and of the first and second nickel layers. The distance between the other (111) nickel layers is the calculated bulk value $d=2.028$ Å. The minimum energy is finally calculated for the different models when all the atoms have reached their equilibrium positions. The results for the atomic structure are given in Table I, where we have reported the equilibrium values for the distance d_0 between the graphene layer and the Ni(111) surface, and the distances d_1 and d_2 between the first three layers of the nickel substrate. The calculated energy for the different models is also given in this table. A short inspection of these results shows that model C is the most favorite configuration, in agreement with LEED and ICISS experimental conclusions.[6,7] We found that the energy is, respectively, 62 meV and 66 meV higher for model A and model B than for model C. These energy differences are comparable to k_BT, where T is the temperature found in the literature for the synthesis of the interface. No appreciable buckling between the two nonequivalent carbon atoms was found in our calculation and the calculated distance between the graphene layer and the substrate (about 2.12 Å) is very close to the measured value.[6,7] As expected, this calculated distance is nearly the same for model B and model C, but the energy difference found between these two models shows that nickel atoms of the second and third layers also interact (even if weakly) with the graphene layer. The rather high equilibrium distance between the graphene layer and the substrate found for model A

TABLE I. Results for the atomic structure of the three graphene/Ni(111) interface models and for the clean Ni(111) surface: d_0 is the distance between the graphene overlayer and the interface nickel layer (the two values for the two nonequivalent carbon atoms are indicated); d_1 is the distance between the interface nickel layer and the second nickel layer; d_2 is the distance between the second and third nickel layers; ΔE is the energy difference between the energy calculated for the different slabs and the energy calculated for model C; m is the interface/surface nickel spin magnetic moment.

	Ni(111)	Model A	Model B	Model C
d_0 (Å)		3.050/3.050	2.113/2.120	2.122/2.130
d_1 (Å)	2.006	1.975	2.034	2.011
d_2 (Å)	2.029	1.999	2.015	2.014
ΔE (eV)		+0.062	+0.066	0.000
m (μ_B)	0.716	0.673	0.514	0.553

(about 3.0 Å) indicates that the electronic structure of graphene will not be strongly modified by the nickel surface in this configuration.

IV. ELECTRONIC AND MAGNETIC STRUCTURE OF THE GRAPHENE/Ni(111) INTERFACE

Results for the nickel magnetic moment as a function of the distance from the interface are shown in Fig. 2 for the three interface models. These results are also compared in the same figure with those calculated for the clean Ni(111) surface. For each of these systems, the interface (or the surface) is on the right-hand side of the figure while the center of the slab is on the left-hand side. The horizontal dashed line refers to the calculated magnetic moment of bulk nickel (0.66 μ_B). The magnetic moment is evaluated from the difference between majority and minority spin electrons inside the atomic spheres. Its absolute value depends of course on the chosen atomic sphere radius. The most important information in Fig. 2 is the relative variation of the magnetic moment for the top nickel layer when compared to the bulk value. For the two models with carbon atoms just above the interface nickel atoms (model C and model B), the magnetic moment shows a reduction of 16% and 22%, respectively, while for model A the magnetic moment is slightly enhanced (+2%). This enhancement is lower than in the case of the clean Ni(111) surface (+7%). For the three interface models and for the clean surface slabs, the magnetic moment converges to the same value (0.67 μ_B) in the center of the slabs. The small discrepancy of 0.01 μ_B found between this value and the calculated bulk value can be due to the different k-meshes used in the slab (two-dimensional mesh) and in the bulk (three-dimensional mesh) calculations. In accordance with the results of Grad *et al.* in the case of the h-BN/Ni(111) interface,[11] we have observed oscillations of the magnetic moment in the slabs, with amplitude of 0.45% and a period of 6–8 layers. These oscillations can also contribute to the $0.01\mu_B$ discrepancy between the magnetic moment in the center of the slab and the bulk value.

In Fig. 3 is reported the majority spin band structure of four different systems: the clean Ni(111) slab (a), the graphene monolayer (b), the slab terminated by graphene/Ni(111) interfaces with the same atomic structure as for model A (c) and with the same atomic structure as for model C (d). The band structure for model B is very similar to that of model C and is not shown here. The band structure shown in Fig. 3(a) has been calculated with a 13 nickel layer slab and we have checked, with a thicker 19 nickel layer slab, that all the features represented in Fig. 3(a) are accurately calculated. In particular, the surface state whose energy at $\bar{\Gamma}$ is close to the Fermi energy E_F is perfectly reproduced. This surface state, which has predominantly s and p characters,

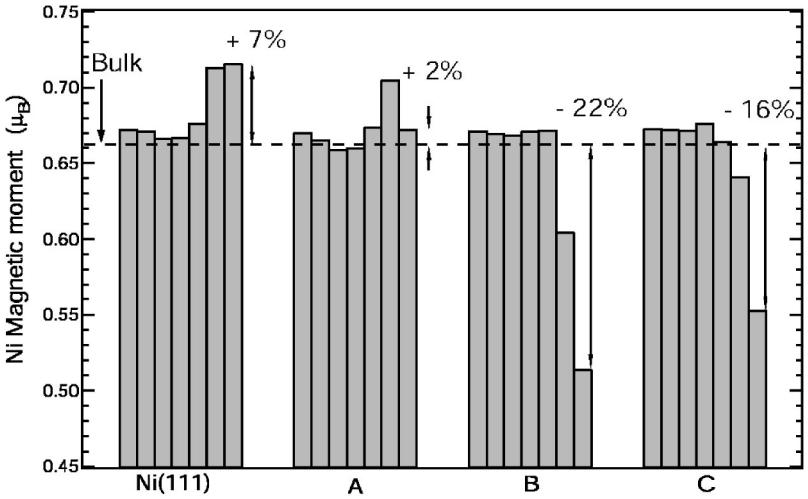

FIG. 2. Calculated nickel magnetic moment for the three models of the graphene/Ni(111) interface and for the clean Ni(111) surface. For each system, the magnetic moment is plotted for the successive nickel layers from the center of the slab (left side) to the surface/interface (right side). The horizontal dashed line is the value calculated for bulk nickel. The difference between the interface/surface magnetic moment and the bulk value is indicated.

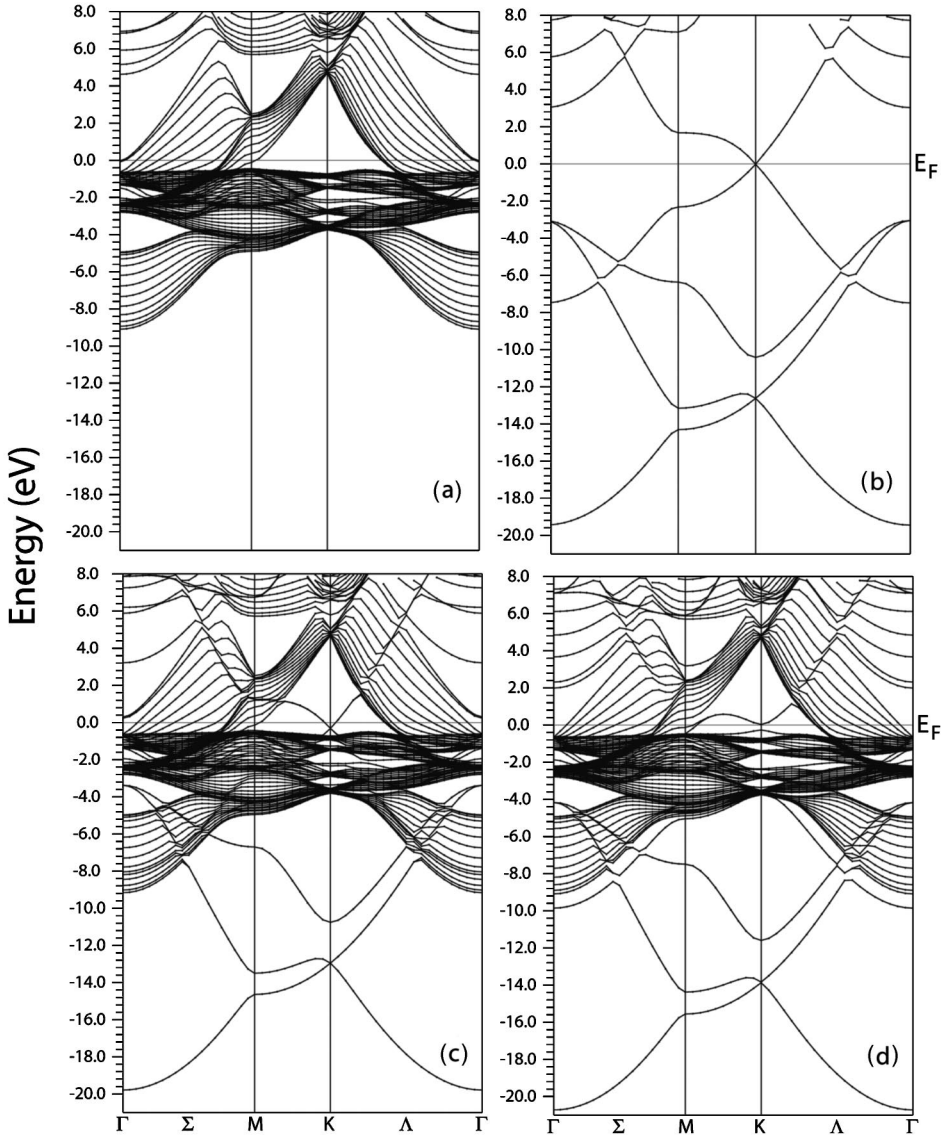

FIG. 3. Calculated majority spin band structure for: a clean Ni(111) slab (a), a graphene monolayer (b), a slab terminated by graphene/Ni(111) interfaces with the same atomic structure as for model A (c), and with the same atomic structure as for model C (d).

has been observed in inverse photoemission experiments.[18,19] The two unoccupied states whose energy at $\bar{\Gamma}$ is, respectively, 4.63 eV and 5.16 eV correspond to the image state, which has been observed experimentally at about 4.6 eV above E_F.[17,18] The rather good agreement between the calculated and measured image state energy is surprising because the DFT-GGA used in our calculation cannot reproduce the exact shape of the image potential in the vacuum and far from the surface.[20] The splitting of the image state is an artefact of the slab method used in our calculation (the wave function for this image state extends rather far in the vacuum side of the surface and a small overlap between image state wave functions across the 22 a.u. vacuum layer can hardly been avoided). The flat band above the splitted image state refers to the bulk projected band structure. Finally, we note the presence of occupied surface states with predominantly *d* character (and with a small mixing with *p* orbitals) in the three bulk gaps at the $\bar{K}$ point. Similar states were found in a tight-bind calculation by Tersoff and Falicov.[21] These states, whose energy is close to the Fermi energy, may hybridize with the π states of graphene.

The band structure for graphene shown in Fig. 3(b) is actually calculated for a periodic structure where graphene monolayers are separated by the same vacuum distance as for the graphene/Ni(111) slabs. This band structure shows the crossing of the π and π^* bands at the $\bar{K}$ point and at the Fermi energy (graphene is a semimetal) as well as the flat unoccupied σ^* band at about 8.0 eV above E_F. Figure 3(b) also shows two additional parabolic bands, with their minima at $\bar{\Gamma}$ and at energies 3.02 eV and 5.73 eV above the Fermi energy. These two spurious bands, which are not shown in the band structure of graphene presented by Souzu *et al.*,[9] are due to the residual interaction between adjacent graphene monolayers in our calculation (slab structure artefact). The wave functions which correspond to these unoccupied spuri-

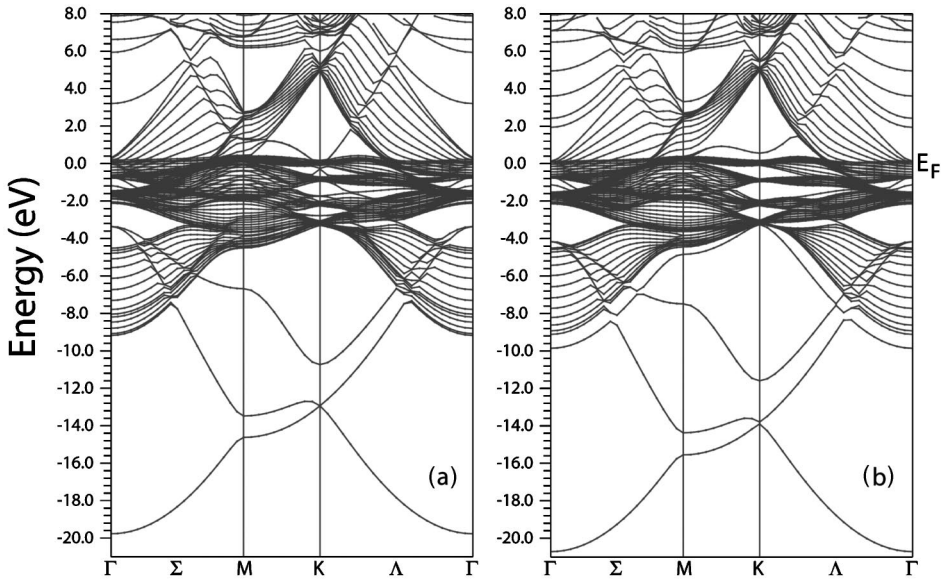

FIG. 4. Calculated minority spin band structure for: a slab terminated by graphene/Ni(111) interfaces with the same atomic structure as for model A (a), and with the same atomic structure as for model C (b).

ous states are maximal in the vacuum space between graphene layers.

The majority spin band structure for the slab terminated by graphene/Ni(111) interfaces with the same atomic structure as for model A is represented in Fig. 3(c). This band structure shows negligible differences with respect to the superimposed band structures of graphene and clean Ni(111) slab. This proves that the interaction between the metal substrate and the carbon overlayer is weak because of the rather large equilibrium distance between the graphene and interface nickel layers. The only modifications of the graphene bands induced by this weak interaction consist in a rigid 0.35 eV downward shift of the graphene bands with respect to E_F. This shift is consistent with the charge transfer from nickel to graphene, which has previously been predicted in a paramagnetic calculation for model A.[10] Note that the spurious bands found in the band structure of graphene are the only ones not shifted with respect to E_F. The only nickel state modification induced by the weak interaction with the carbon layer concerns the nickel surface and image states. Figure 3(c) shows indeed a small upward shift of the nickel surface state, just above the Fermi energy at the $\bar{\Gamma}$ point. The wave function for this surface state reaches its maximal values in the vicinity of the top nickel layers and presents an exponentially decaying tail, the amplitude of which is small at the distance of 3.05 Å from the interface nickel. This is the reason why this state, even if shifted, still exists in the presence of the overlayer for model A. The GGA equivalent of the image state, which was observed for the clean nickel slab, is not present when the graphene layer covers the surface. The minority spin band structure for the nickel slab with model A for the interface atomic structure is represented in Fig. 4(a). It is very similar to that of the majority spin except from an upward shift of the nickel derived bands. The minority spin graphene π and π^* bands still cross each other at the $\bar{K}$ point, but the crossing point of these two bands, which was located above the nickel *d* bands for the majority spin, is located in one of the nickel *d* band gaps for the minority spin.

The majority spin band structure for the slab terminated by graphene/Ni(111) interfaces with the same atomic structure as for model C is represented in Fig. 3(d). We have seen that the total energy is lower for this system because of the strong interaction between the carbon layer and the substrate. As a clear evidence of this strong interaction, Fig. 3(d) shows noticeable modifications of the graphene and nickel band structure. The first modification consists of a nonrigid downward shift of the occupied graphene bands: at the $\bar{\Gamma}$ point, the π band is shifted by 2.35 eV while the σ band is only shifted by 1.25 eV. These values are in very good agreement with the photoemission measurements of Nagashyma *et al.*[22] The unoccupied σ^* band is also shifted by 1.11 eV. The interaction between graphene and metal layers implies a hybridisation of the graphene π bands with the nickel *d* bands (and secondary with the nickel *s* and *p* bands) as shown in Fig. 5. In particular, three occupied and one unoccupied interface states, with a strong contribution of the carbon p_z orbitals (the O_z axis being perpendicular to the interface), are clearly visible near the $\bar{K}$ point. The three occupied interface states, which we labelled I_1, I_2 and I_3, have the energies −3.37 eV, −2.40 eV, and −0.20 eV, respectively. The unoccupied interface state I_4 is just above the Fermi energy (0.02 eV). The interface states I_3 and I_4 result from a 0.22 eV gap opening between the graphene occupied π and unoccupied π^* bands at the $\bar{K}$ point. These interface states correspond probably to the states which are found experimentally by Nagashyma *et al.*[22] The interface states I_2 and I_4 can be attributed to the carbon atoms just above the interface nickel atoms (C_1 carbon atoms), while the states I_1 and I_3 only involve the carbon atoms C_2. Another interface state (I_5) is clearly visible near the $\bar{M}$ point of the Brillouin zone at 3.18 eV. This state results from a hybridisation of the

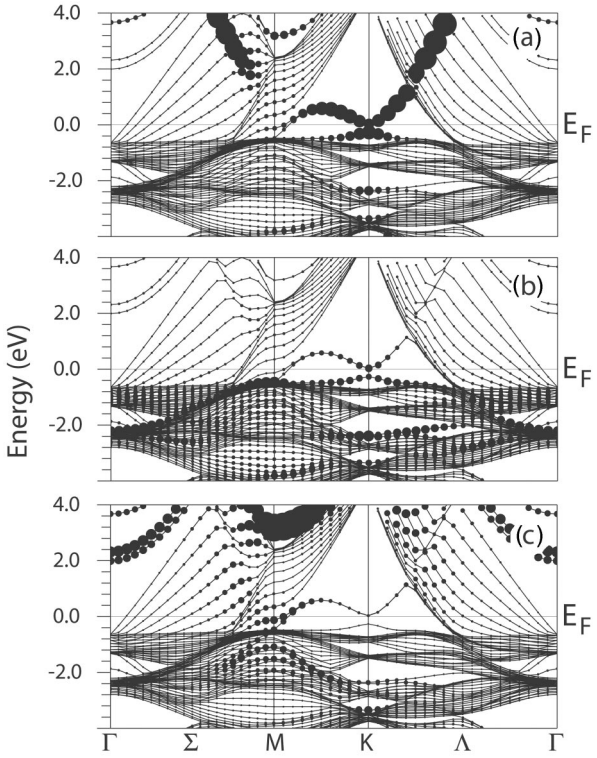

FIG. 5. Calculated majority spin band structure for a slab terminated by graphene/Ni(111) interfaces with the same atomic structure as for model C. The radius of the circles is proportional to the partial p_z density of states of the two carbon atoms (a), to the partial *d* density of states of the interface nickel atoms (b), and to the partial *s* and *p* density of states of the interface nickel atoms (c). For a better clarity, the radius of the circles has actually been multiplied by 5.0 in (a) and by 10.0 in (c).

interface nickel p_x, p_y, and *d* orbitals with carbon p_z orbitals. Other unoccupied states which mix the *s*, p_z and *d* nickel orbitals with the *s* (and a small minority of p_z) carbon orbitals are also formed in the gap near the $\bar{\Gamma}$ point at about 2.0 eV. We cannot say if these states, which extend rather far in the vacuum layer, originate from a coupling between the clean nickel surface state and graphene states or if they are only spurious inter slab states. In Fig. 6 we plotted the density of states for the three occupied I_1, I_2, and I_3 and the two unoccupied I_4 and I_5 interface states. The densities are plotted in the plane perpendicular to the interface and which contains the two nonequivalent carbon atoms C_1 and C_2 (this plane is indicated by a dotted line in Fig. 1).

Figure 6 shows that the corresponding wave functions are located in the vicinity of the interface (mainly in the graphene layer and in the top and second nickel layers), with no contribution from the nickel atoms in the center of the slab. As shown in this figure, the different interface states correspond to: bonding between carbon atoms C_2 and interface nickel atoms (I_1), bonding between carbon atoms C_1 and interface nickel atoms (I_2), antibonding between carbon atoms C_2 and interface nickel atoms (I_3), and antibonding between carbon atoms C_1 and interface nickel atoms (I_4). The interface state I_5, which involves the nickel atoms and the carbon atoms C_2 and C_1, corresponds to a bonding orbital between the two carbon atoms. The minority spin band structure for this slab is represented in Fig. 4(b). Its lowest occupied graphenelike bands have exactly the same energy as those of the majority spin. Differences with majority spin band structure appear for the nickel bands, which are shifted upwards, and for the interface states. Minority spin interface states I_1, I_2, and I_3 are located just at the edge of the substrate energy gaps, near the $\bar{K}$ point and at the energies −3.24 eV, −1.96 eV, and 0.18 eV (the interface state I_3 is unoccupied for minority spin). The unoccupied minority spin interface states I_4 and I_5 have the energies 0.57 eV and 3.32 eV, respectively. The different behavior of the majority and minority spin interface states explains why the carbon layer possesses a small magnetic moment ($-0.01\ \mu_B$ and $0.02\ \mu_B$ for C_1 and C_2, respectively). Note that the magnetic splitting of the unoccupied interface states (about 0.55 eV for I_4 and 0.14 eV for I_5) is smaller than the energy difference between these two kinds of states (about 3.0 eV). This means that the contributions from these different interface states may be easier to separate than the contributions from minority and majority spin in an EELS experiment.

V. EELS SPECTRA AT THE GRAPHENE/Ni(111) INTERFACE

The *K*-edge EELS spectra calculated within the dipole approximation for the interface carbon atoms (model C) as well as for a graphene sheet and bulk graphite are shown in Fig. 7. The spectra shown in this figure are calculated for the scattering vector **q** parallel and perpendicular to the graphene layer. The integrated spectra, which correspond to an averaging over all the possible directions for **q**, are also shown in this figure.

Experimental broadening of the spectra has been taken into account by a convolution with a 1.0 eV full width at half maximum Gaussian function. The main peaks of the graphene spectrum (at 1.9 eV and 8.3 eV above E_F) correspond, respectively, to transitions to the π^* and σ^* bands. The inter layer spurious states do not give significant contribution to the graphene spectra. Indeed, the matrix elements which describe transitions between the initial carbon core state and one of these spurious states are very small because the wave functions for inter graphene states is maximal in the vacuum region between graphene layers and negligible near the carbon atoms. The π^* bands are modified by the interaction with the nickel magnetic substrate. The first peak of the interface carbon spectra (at about 0.8 eV) corresponds to the interface state I_4. The second peak, near 3.0 eV, mainly comes from the unoccupied interface state I_5 at the $\bar{M}$ point. The contribution from the interface states, which have energy of about 2.1 eV at the $\bar{\Gamma}$ point, is not very important. The small magnetic splitting between majority and minority spin that has been calculated cannot be observed in the main peaks of Fig. 7 because of the 1.0 eV broadening which has been used to calculate the spectra. The σ^* peak is shifted to 7.3 eV for the carbon atoms at the interface. The detailed shape of the spectra between 10.0 eV and 25.0 eV is also severely modified by the interaction with the other graphene

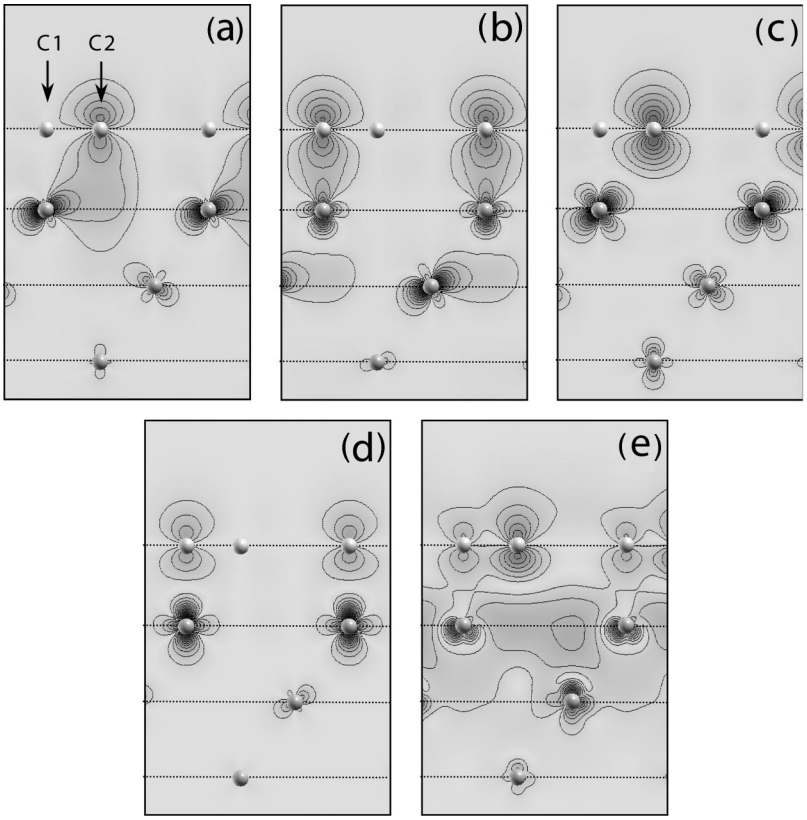

FIG. 6. Calculated majority spin local density of states for the $\bar{K}$ point interface states I_1 (a), I_2 (b), I_3 (c), and I_4 (d) and for the $\bar{M}$ point interface state I_5 (e). The grey levels are proportional to $r[\rho(r)]^{1/2}$.

layers (in graphite) or with the nickel layers (for the interface), as can be seen in Fig. 7.

VI. CONCLUSION

The atomic and the electronic structure of the graphene/Ni(111) interface have been studied with a first-principles calculation. For the lowest energy structure, carbon atoms are located just above interface nickel atoms as well as in the fcc hollow sites, at a distance of 2.13 Å from the top Ni layer. We found that the interaction with the graphene overlayer is responsible for a 16% reduction of the interface nickel magnetic moment. Several occupied and unoccupied interface states have been identified and we have shown that the later manifest themselves by noticeable modifications of the carbon *K*-edge EELS spectrum.

ACKNOWLEDGMENTS

This work was supported by the European Research Training Network New Fullerenelike Materials, Contract No. HPRN-CT-2002-00209. The calculations presented in this article have been performed on the CALMIP/UPS Toulouse parallel computer center.

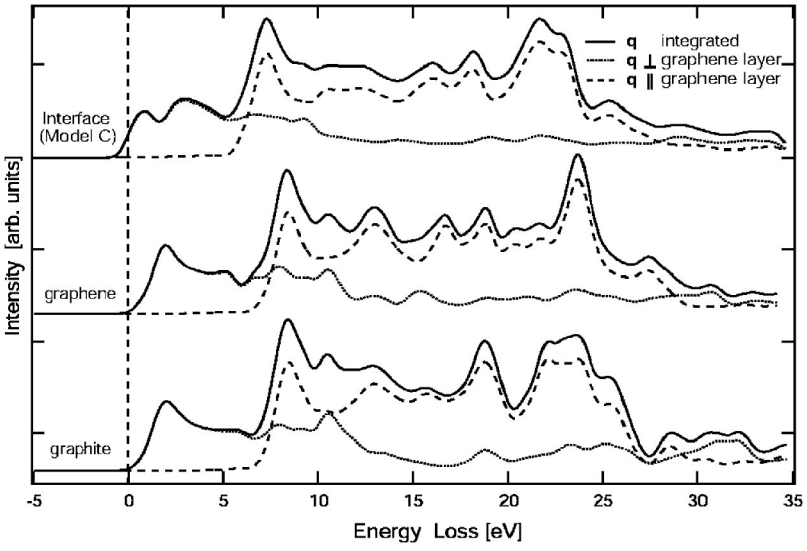

FIG. 7. *K*-edge EELS spectra for: interface carbon atoms with model C for the atomic structure (top curve), a graphene carbon atom (centre curve), and a graphite carbon atom (bottom curve). The solid lines refer to the averaged spectra for which the transferred momentum **q** describes the whole space (4π solid angle). Contributions to these spectra with transferred momentum **q** perpendicular and parallel to the graphene layer are shown as dotted and dashed lines, respectively. In the spectra the Fermi energy E_F corresponds to the energy zero.

[1] A. M. Shikin, D. Farías, V. K. Adamchuk, and K.-H. Rieder, Surf. Sci. **424**, 155 (1999).
[2] Hu Zi-pu, D. F. Ogletree, M. A. Van Hove, and G. A. Somorjai, Surf. Sci. **180**, 433 (1987).
[3] T. Aizawa, R. Souda, S. Otani, Y. Ishizawa, and C. Oshima, Phys. Rev. B **42**, 11469 (1990).
[4] D. Ugarte, A. Châctelain, and W. A. de Heer, Science **274**, 5294 (1996); **274**, 1897 (1996).
[5] G. E. Gadd, M. Collela, M. Blackford, A. Dixon, P. J. Evans, D. McCulloch, S. Bulcock, and D. Cockayne, Carbon **39**, 1769 (2001).
[6] Y. Gamo, A. Nagashima, M. Wakabayashi, M. Terai, and C. Oshima, Surf. Sci. **374**, 61 (1997).
[7] H. Kawanowa, H. Ozawa, T. Yakazi, Y. Gotoh, and R. Souda, Jpn. J. Appl. Phys., Part 1 **41**, 6149 (2002).
[8] R. Rosei, M. De Crescenzi, F. Sette, C. Quaresima, A. Savoia, and P. Perfetti, Phys. Rev. B **28**, 1161 (1983).
[9] Y. Souzu and M. Tsukada, Surf. Sci. **326**, 42 (1995).
[10] K. Yamamoto, M. Fukushima, T. Osaka, and C. Oshima, Phys. Rev. B **45**, 11358 (1992); **45**, 11358 (1992).
[11] G. B. Grad, P. Blaha, K. Schwarz, W Auwärter, and T. Greber, Phys. Rev. B **68**, 085404 (2003).
[12] F. Pailloux, D. Imhoff, T. Sikora, A. Barthélémy, J. L. Maurice, J. P. Contour, C. Colliex, and A. Fert, Phys. Rev. B **66**, 014417 (2002).
[13] S. Fabris, S. Nufer, C. Elsasser, and T. Gemming, Phys. Rev. B **66**, 155415 (2002).
[14] A. Falqui, V. Serin, L. Calmels, E. Snoeck, A. Corrias, and G. Ennas, J. Microsc. **210**, 80 (2003).
[15] P. Blaha, K. Schwarz, G. K. H. Madsen, D. Kvasnicka, and J. Luitz, WIEN2k, an augmented plane wave+local orbitals program for calculating crystal properties, Vienna University of Technology, Vienna, 2001.
[16] J. P. Perdew, S. Kurth, A. Zupan, and P. Blaha, Phys. Rev. Lett. **82**, 2544 (1999).
[17] G. Nicolay, F. Reinert, S. Hüfner, and P. Blaha, Phys. Rev. B **65**, 033407 (2001).
[18] S. Yang, K. Garrison, and R. A. Bartynski, Phys. Rev. B **43**, 2025 (1991); **43**, 2025 (1991).
[19] M. Donath, Surf. Sci. Rep. **20**, 251 (1994).
[20] N. D. Lang and W. Kohn, Phys. Rev. B **1**, 4555 (1970).
[21] J. Tersoff and L. M. Falicov, Phys. Rev. B **26**, 11 (1982); **26**, 6186 (1982).
[22] A. Nagashima, N. Tejima, and C. Oshima, Phys. Rev. B **50**, 17487 (1994); **50**, 17487 (1994).